Inorganic Chemistry

Communication

pubs.acs.org/IC

$ReBe_2B_5O_{11}$ (Re = Y, Gd): Rare-Earth Beryllium Borates as Deep-Ultraviolet Nonlinear-Optical Materials

Xue Yan,[†,‡,§] Siyang Luo,*[,†,‡] Zheshuai Lin,*[,†,‡] Jiyong Yao,[†,‡] Ran He,[†,‡] Yinchao Yue,[†,‡] and Chuangtian Chen[†,‡]

[†]Beijing Center for Crystal Research and Development, Technical Institute of Physics and Chemistry, Chinese Academy of Sciences, Beijing 100190, China

[‡]Key Laboratory of Functional Crystals and Laser Technology, Technical Institute of Physics and Chemistry, Chinese Academy of Sciences, Beijing 100190, China

[§]National Key Laboratory of Advanced Functional Composite Materials, Aerospace Research Institute of Materials & Processing Technology, Beijing 100076, China

Supporting Information

ABSTRACT: Two novel rare-earth beryllium borates $ReBe_2B_5O_{11}$ (*Re* = Y, Gd) have been discovered. These materials possess a unique structural feature with a platelike infinite $^2_\infty[Be_2B_5O_{11}]^{3-}$ superlayer, which is first found in beryllium borates. The superlayer can be seen as sandwich-shaped with $^1_\infty[B_4O_8]^{4-}$ chains linking up with a $^2_\infty[Be_2BO_5]^{3-}$ sublayer above and below via the B−O−Be bond. Each $^2_\infty[Be_2B_5O_{11}]^{3-}$ layer is further connected to the neighboring layer through Re^{3+} cations coordinating with O atoms. Both of these two crystals have very short cutoff wavelengths below 200 nm and exhibit relatively large nonlinear-optical (NLO) effects, indicating their promising applications as good deep-UV NLO crystals.

The generation of deep-ultraviolet (deep-UV) coherent light (wavelength below 200 nm) has become increasingly important for their wide applications in laser science and technology including areas such as ultrafine spectral analysis, precise micromanufacture, and photochemistry.[1] The one best way to generate deep-UV coherent light with solid-state lasers is through a cascaded frequency conversion using nonlinear-optical (NLO) crystals.[2] However, few NLO crystals can generate coherent laser in the deep-UV region to overcome the handicap described as a "200-nm wall"[3] because it is very difficult to find suitable materials that possess both short UV absorption cutoff wavelength (λ_{cutoff} < 200 nm) and large optical anisotropy [e.g., NLO coefficients ~0.39 pm/V as in KH_2PO_4 (KDP) and birefringence Δn > 0.07]. So far, $KBe_2BO_3F_2$ (KBBF) is the sole NLO crystal that can practically produce the deep-UV harmonic generation (d_{11} = 0.47 pm/V, λ_{cutoff} = 150 nm, and $\Delta n \sim 0.08$) and has been applied in many advanced scientific instruments.[1b,4] However, thick KBBF crystal is hard to grow because of its strong layer habit, which heavily limits its wide applications. To further explore good deep-UV NLO crystals, many attempts have been performed in beryllium borates[5] because the tetrahedral BeO_4 group can be connected to BO_3 and/or BO_4 groups to form various beryllium borate fundamental building blocks (FBBs) with strong deep-UV NLO responses, such as $[Be_2BeO_{11}]^{9-}$, $[Be_2BO_5]^{3-}$, $[Be_3B_3O_{12}F]^{10-}$, and $[Be_2BO_3F_2]^-$. Recently, a few new beryllium borates have been discovered as potential deep-UV NLO materials, including $RbBe_2BO_3F_2$, $Sr_2Be_2B_2O_7$, $NaBeB_3O_6$, $ABe_2B_3O_7$ (A = K, Rb), $NaCsBe_6B_5O_{15}$, $NaSr_3Be_3B_3O_9F_4$, $NaCaBe_2B_2O_6F$, and $M_3Be_2B_5O_{12}$ (*M* = Sr, Ba).[5]

So far, in all reported beryllium borate UV NLO materials, the A-site cations have been restricted to the alkaline and/or alkaline-earth cations. The study on rare-earth beryllium borates is lacking. In general, the UV absorption edges of rare-earth compounds are hardly down to the deep-UV region because of the optical absorption caused by the *d*−*d* or *f*−*f* electronic transition. However, the rare-earth cations Y^{3+} or Gd^{3+} can transmit the deep-UV light because their full-occupied *d* ($3d^{10}$) or half-occupied *f* ($4f^7$) electronic shells effectively inhibit the unfavorable electronic transitions. This is clearly demonstrated by the fact that the short cutoff wavelengths are down to the deep-UV region in the rare-earth borates $YAl_3(BO_3)_4$ (YAB)[6] and $ReCa_4O(BO_3)_3$ (*Re* = Y, Gd).[7] Moreover, the rare-earth cations are usually coordinated with O atoms to form a distorted metal oxide polyhedron with large hyperpolarizability, which is helpful to increase the second-harmonic-generation (SHG) responses, as shown in the case of YAB.[8] Therefore, in this study we chose the rare-earth cations Y^{3+} or Gd^{3+} and first synthesized two novel rare-earth beryllium borates, $ReBe_2B_5O_{11}$ (*Re* = Y, Gd), which exhibit new structural characteristics. The linear-optical and NLO properties and chemical and thermal stabilities of $ReBe_2B_5O_{11}$ were determined. The combination of experiments and first-principles studies reveals that these rare-earth beryllium borates have very good NLO properties in the deep-UV region. This clearly demonstrates that the incorporation of rare-earth cations with full- or half-occupied *d* or *f* electronic shells in beryllium borates may provide an additional way to explore novel deep-UV NLO crystals.

Colorless block single crystals of $ReBe_2B_5O_{11}$ (*Re* = Y, Gd) were grown through a spontaneous nucleation method from the melt of a Re_2O_3−BeO−B_2O_3−Li_2O mixture. After $ReBe_2B_5O_{11}$ single crystals were obtained (Figure S1 in the SI), single-crystal X-ray diffraction (XRD) measurements were performed (Table

Received: November 27, 2013
Published: January 28, 2014

dx.doi.org/10.1021/ic4029436 | *Inorg. Chem.* 2014, 53, 1952−1954

S1 in the SI). The experimental powder XRD patterns were found to be in good agreement with the calculated ones based on the single-crystal crystallographic data (Figure S2 in the SI).

The $ReBe_2B_5O_{11}$ compounds are isostructural and crystallize in orthorhombic crystal systems with an acentric space group of $Pna2_1$ (atomic coordinates, isotropic displacement coefficients, and bond lengths are listed in Tables S2−S7 in the SI). Both materials feature layer structures composed of the platelike infinite superlayer $^2_\infty[Be_2B_5O_{11}]^{3-}$ (Figure 1a), and this is the first

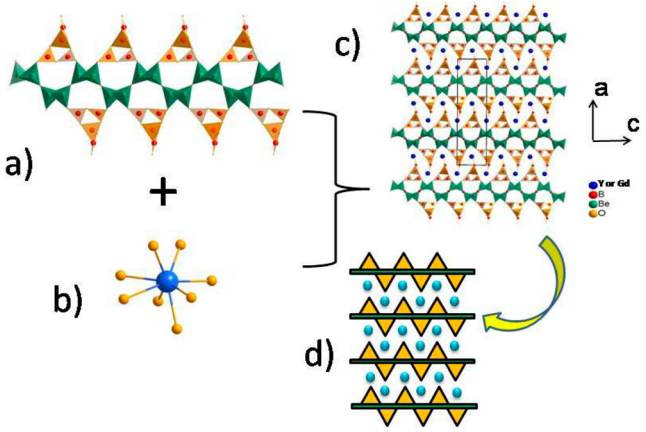

Figure 1. Schematic of the $YBe_2B_5O_{11}$ and $GdBe_2B_5O_{11}$ structures. (a) Polyhedral view of a superlayer $^2_\infty[Be_2B_5O_{11}]^{3-}$. (b) Ball-and-stick model for $Y{-}O_8$ ($Gd{-}O_8$) coordination. (c) Overall structure projected along the *b* axis. BeO_4 tetrahedra are shown in green; triangular BO_3 and tetrahedral BO_4 units are shown in yellow. The Y (Gd), Be, B, and O atoms are shown as blue, green, red, and yellow spheres, respectively. (d) Sketch of the layer structure. Yellow triangles stand for $[B_4O_8]^{4-}$ anion groups, green strips stand for $^2_\infty[Be_2BO_5]^{3-}$ sublayers, and blue circles stand for Y (Gd) cations.

time for this to be observed in borates. Each $^2_\infty[Be_2B_5O_{11}]^{3-}$ layer is further connected to the neighboring superlayer through Re^{3+} cations coordinating with O atoms (Figure 1b−d). This layer feature in $ReBe_2B_5O_{11}$ is strongly in favor of the increasing anisotropy of this sort of material, which is beneficial to the strong SHG response as well as the large birefringence satisfying the phase-matching condition.[2] To further describe the structural features, $YBe_2B_5O_{11}$ will be discussed in detail as representations.

Each $^2_\infty[Be_2B_5O_{11}]^{3-}$ superlayer (Figure 2a) can be seen as a sandwich shape with $^1_\infty[B_4O_8]^{4-}$ chains (Figure 2b) linking up with a $^2_\infty[Be_2BO_5]^{3-}$ sublayer (Figure 2c) above and below via the B−O−Be bond along the *a* axis. The FBB of a straight $^1_\infty[B_4O_8]^{4-}$ chain is composed of three triangular BO_3 groups and a BO_4 tetrahedron interconnected via sharing corners, which is the first found in borates. The $^2_\infty[Be_2BO_5]^{3-}$ sublayer consists of planar BO_3 units connected with BeO_4 tetrahedra and is zigzaged along the *c* axis (Figure 2d). The B−O bond distances of the BO_3 and BO_4 groups are in the ranges of 1.337(8)−1.414(9) and 1.460(8)−1.478(8) Å, respectively. The BeO_4 group has a Be−O distance ranging from 1.590(1) to 1.670(1) Å. All of the B−O and Be−O bond lengths are comparable to those of other beryllium borate compounds. The Y atoms interconnect with O to form Y−O chains along the *b* axis (Figure 2e). Each Y^{3+} cation is coordinated by eight O atoms to form a deformed (YO_8) polyhedron with Y−O bond distances in the range of 2.287−2.719 Å.

UV−vis−near-IR diffuse-reflectance spectra (Figure S3 in the SI) observed no obvious absorption peak in the range of 200−

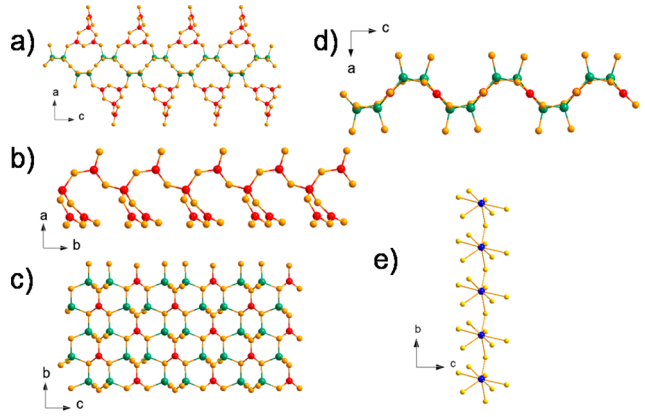

Figure 2. Detailed geometries of groups in $YBe_2B_5O_{11}$. (a) $^2_\infty[Be_2B_5O_{11}]^{3-}$ superlayer projected along the *b* axis. (b) Graph of the $^1_\infty[B_4O_8]^{4-}$ chain projected along the *c* axis. (c) $^2_\infty[Be_2BO_5]^{3-}$ sublayer projected along the *a* axis. (d) $^2_\infty[Be_2BO_5]^{3-}$ sublayer projected along the *b* axis. (e) Y−O chain projected along the *a* axis.

2500 nm in $ReBe_2B_5O_{11}$, indicating that their UV cutoff edge is lower than 200 nm. The curves of the SHG signal as a function of the particle size for $YBe_2B_5O_{11}$ and $GdBe_2B_5O_{11}$ were detected and compared with that of KDP (Figure 3). It was shown that the

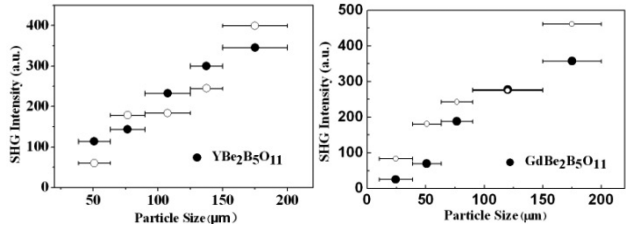

Figure 3. Powder SHG intensity measurements of $YBe_2B_5O_{11}$ (left) and $GdBe_2B_5O_{11}$ (right). The sieved KDP powders (○) were used as a reference.

SHG signals of both crystals are as strong as that of KDP and consistent with the phase-matching behavior according to the rule proposed by Kurtz and Perry.[9] The above optical measurements demonstrate that $ReBe_2B_5O_{11}$ have very good deep-UV NLO properties.

Differential scanning calorimetry (DSC) measurements were carried out with ground crystals of $ReBe_2B_5O_{11}$ (Figure S4 in the SI). The DSC curves for $YBe_2B_5O_{11}$ exhibit two endothermic peaks upon heating to 1250 °C. There are two endothermic peaks on the heating curve at 1037 and 1157 °C. The powder XRD patterns showed that the first endothermic peaks are decomposition and the following peaks are melting of the residues. As for $GdBe_2B_5O_{11}$, there was only one endothermic peak of decomposition at 1065 °C as the sample was being heated to 1300 °C. XRD data of the $YBe_2B_5O_{11}$ or $GdBe_2B_5O_{11}$ residues in the platinum pan after melting showed that they decomposed into YBO_3 or $GdBO_3$, respectively. The results demonstrate that $ReBe_2B_5O_{11}$ are incongruently melting compounds. The title compounds are nonhygroscopic and acid-resistant. No etching was observed after immersion in water or dilute acid for 1 week.

The electronic structures in $ReBe_2B_5O_{11}$ are calculated by the first-principles theory. Partial density of states (Figure S5 in the SI) reveals that the upper part of the valence band is dominated by O and the contribution from B is also significant, while the

dx.doi.org/10.1021/ic4029436 | Inorg. Chem. 2014, 53, 1952−1954

bottom of the conduction band is mainly composed of the *Re d* and B 2*p* orbitals. This means that both *Re* cations and B−O groups may have a significant influence on the optical properties.

According to the electronic band structure, the SHG coefficients are calculated.[10] They are d_{31} = 0.08 pm/V, d_{32} = 0.42 pm/V, and d_{33} = −0.67 pm/V for $YBe_2B_5O_{11}$ and d_{31} = 0.20 pm/V, d_{32} = 0.43 pm/V, and d_{33} = −0.80 pm/V for $GdBe_2B_5O_{11}$. Their powder SHG effects are estimated to be 0.9KDP and 1.1KDP, respectively, according to the Kurtz and Perry method,[9] which are in very good agreement with the experimental results.

In order to elucidate the mechanism of the optical properties in rare-earth beryllium borates, atom-cutting analysis[11] is performed for $YBe_2B_5O_{11}$ as an example (listed in Table 1),

Table 1. SHG Coefficients of $YBe_2B_5O_{11}$ from the Atom-Cutting Method

	YO_8	BO_3	BO_4	BeO_4	original value
d_{31} (pm/V)	0.083	−0.004	−0.003	−0.030	0.080
d_{32} (pm/V)	0.235	0.360	0.040	0.030	0.420
d_{33} (pm/V)	−0.390	−0.480	−0.080	−0.020	−0.675

which clearly shows that the BO_3 anionic groups contribute about 60% to the overall SHG coefficient, while the contributions of BO_4 and BeO_4 tetrahedra are negligibly small. The sum of the SHG coefficients of the respective $[BO_3]^{3-}$, $[BO_4]^{5-}$, and $[YO_8]^{13-}$ anionic groups is larger than the original values. Since some O orbitals are used twice in the atom-cutting procedures.

It is interesting that the contribution of the YO_8 group is about 40% of the overall SHG coefficient. This is inconsistent with the situation in alkaline and alkaline-earth beryllium borates, where the cations almost do nothing to the overall SHG response.[12] It is because the chemical bonds between the Y^{3+} and O^{2-} ions have quite strong covalent characteristics, so the contribution of the YO_8 polyhedra cannot be ignored. For $GdBe_2B_5O_{11}$, the same conclusion can be obtained; i.e., its SHG effects mainly attribute to the BO_3 and GdO_8 anionic groups (see Table S8 in the SI). The small SHG effect difference (∼20%) in $YBe_2B_5O_{11}$ and $GdBe_2B_5O_{11}$ is mainly attributed to the covalency effect in the YO_8 and GdO_8 polyhedra. However, it should be noted that the SHG effect in $YBe_2B_5O_{11}$ is much smaller than that of YAB (d_{11} = 1.7 pm/V). Since the structural distortion of YO_8 in the former is not as strong as that of YO_6 in the latter. Therefore, it will be a goal in future studies to search for novel rare-earth beryllium borates with more distorted polyhedra in order to enhance the SHG response.

In conclusion, two new rare-earth beryllium borate compounds $ReBe_2B_5O_{11}$ (*Re* = Y, Gd) were obtained for the first time. They feature a novel anionic superlayer $^2_\infty[Be_2B_5O_{11}]^{3-}$, which consists of the alveolate beryllium borate layer $^2_\infty[Be_2BO_5]^{3-}$ and borate chains $^1_\infty[B_4O_8]^{4-}$. The $^1_\infty[B_4O_8]^{4-}$ chain that extends in a straight line is first found in borates. The short-wavelength absorption edges of both crystals are below 200 nm. A powder SHG test on ground crystals revealed that $YBe_2B_5O_{11}$ and $GdBe_2B_5O_{11}$ are phase-matchable with SHG intensity approximately as large as that of a KDP standard. Our preliminary investigation indicates that the rare-earth beryllium borates $ReBe_2B_5O_{11}$ (*Re* = Y, Gd) have very good deep-UV NLO properties. In addition, it is well-known that rare-earth cations have the capability of producing self-frequency double generation in the NLO crystals, and relevant studies of the title compounds are underway.

■ ASSOCIATED CONTENT

Supporting Information

Crystallographic data in CIF format, experimental and computational methods, tables and figures for crystal characterization, and calculated electronic structures. This material is available free of charge via the Internet at http://pubs.acs.org.

■ AUTHOR INFORMATION

Corresponding Authors

*E-mail: luosy@mail.ipc.ac.cn.

*E-mail: zslin@mail.ipc.ac.cn.

Notes

The authors declare no competing financial interest.

■ ACKNOWLEDGMENTS

This work was supported by the NSF of China (Grants 91022036 and 11174297) and China "973" project (Grants 2010CB630701 and 2011CB922204). The authors acknowledge useful discussion with Pifu Gong.

■ REFERENCES

(1) (a) Savage, N. *Nat. Photonics* **2007**, *1*, 83−85. (b) Cyranoski, D. *Nature* **2009**, *457*, 953. (c) Becker, P. *Adv. Mater.* **1998**, *10*, 979−992. (d) Wu, H. P.; Yu, H. W.; Pan, S. L.; Huang, Z.; Yang, Z. H.; Su, X.; Poeppelmeier, K. R. *Angew. Chem., Int. Ed.* **2013**, *52*, 3406−3410. (e) Wu, H. P.; Yu, H. W.; Yang, Z. H.; Hou, X. L.; Su, X.; Pan, S. L.; Poeppelmeier, K. R.; Rondinelli, J. M. *J. Am. Chem. Soc.* **2013**, *135*, 4215−4218.

(2) Chen, C. T.; Sasaki, T.; Li, R. K.; Wu, Y. C.; Lin, Z. S.; Mori, Y.; Hu, Z. G.; Wang, J. Y.; Aka, G.; Yoshimura, M. *Nonlinear Optical Borate Crystals*; Wiley-VCH: New York, 2012.

(3) Hassaun, J. B. *Laser Fouse World* **1998**, *34*, 127.

(4) (a) Mei, L. F.; Huang, X.; Wang, Y.; Wu, Q.; Wu, B. C.; Chen, C. T. *Z. Kristallogr.* **1995**, *210*, 93−95. (b) Chen, C. T.; Wang, G. L.; Wang, X. Y.; Xu, Z. Y. *Appl. Phys. B: Lasers Opt.* **2009**, *97*, 9.

(5) (a) Chen, C. T.; Luo, S. Y. *J. Opt. Soc. Am. B* **2010**, *26*, 1519−1525. (b) McMillen, C. D.; Hu, J.; Van Derveer, D.; Kolis, J. W. *Acta Crystallogr., Sect. B: Struct. Sci.* **2009**, *65*, 445−449. (c) Chen, C. T.; Wang, Y. B.; Wu, B. C.; Wu, K.; Zeng, W.; Yu, L. *Nature* **1995**, *373*, 322−324. (d) Wang, S. C.; Ye, N.; Li, W.; Zhao, D. *J. Am. Chem. Soc.* **2010**, *132*, 8779−8786. (e) Wang, S. C.; Ye, N. *J. Am. Chem. Soc.* **2011**, *133*, 11458−11461. (f) Huang, H. W.; Yao, J. Y.; Lin, Z. S.; Chen, C. T. *Angew. Chem., Int. Ed.* **2011**, *50*, 9141−9144. (g) Huang, H. W.; Lin, Z. S.; He, R.; Zhai, N.; Chen, C. T. *Chem. Mater.* **2011**, *23*, 5457−5463. (h) McMillen, C. D.; Kolis, J. W. *Inorg. Chem.* **2011**, *50*, 6809−6813.

(6) Chen, X.; Liu, H.; Ye, N. *J. Synth. Cryst.* **2009**, *38*, 544−546.

(7) Iwai, M.; Kobayashi, T.; Furuya, H.; Mori, Y.; Sasaki, T. *Jpn. J. Appl. Phys., Part 2* **1997**, *36*, L276−L279.

(8) He, R.; Lin, Z. S.; Lee, M. H.; Chen, C. T. *J. Appl. Phys.* **2011**, *109*, 103510.

(9) Kurtz, S. K.; Perry, T. T. *J. Appl. Phys.* **1968**, *39*, 3798−3813.

(10) Lin, J.; Lee, M. H.; Liu, Z. P.; Chen, C. T.; Pickard, C. *J. Phys. Rev. B* **1999**, *60*, 13380.

(11) Chen, C. T.; Lin, Z. S.; Wang, Z. Z. *Appl. Phys. B: Lasers Opt.* **2005**, *80*, 1−25.

(12) Kang, L.; Luo, S. Y.; Huang, H. W.; Zheng, T.; Lin, Z. S.; Chen, C. T. *J. Phys.: Condens. Matter* **2012**, *24*, 335503.